A Burst Mode Pulse Density Modulation Scheme for Inductive Power Transfer Systems Without Communication Modules

Shuxin Chen[1], Hongchang Li[2], and Yi Tang[1]
[1]School of Electrical and Electronic Engineering, [2]Energy Research Institute @ NTU
Nanyang Technological University
Singapore
chen1095@e.ntu.edu.sg

***Abstract*—Load voltage regulation in wireless inductive power transfer systems can be achieved by load side control. As the regulation capability of a single converter is limited, a front side converter is usually applied to widen the operation range. Load side information is normally required for the dual side cooperation. However, adding communication modules will inevitably increase the system overall size and cost. Moreover, communication modules have poor reliability and uncertain delay, which may cause difficulties in control. To solve this issue, a burst mode pulse density modulation control scheme is proposed in this paper that can perform output regulation without communication modules and have a high efficiency. Simulation and experimental results are provided in this paper to prove the effectiveness of the proposed method.**

Keywords— Wireless Power Transfer; Voltage Regulation; No communication

I. INTRODUCTION

Wireless inductive power transfer (IPT) systems can transfer power to loads without physical contact, and have become popular due to its superior performances over traditional wired systems, in terms of safety and convenience [1, 2]. A typical IPT system is shown in Fig. 1. A resonator transmits power wirelessly through magnetic fields. There are four basic topologies for the resonator: series-series, series-parallel, parallel-series and parallel-parallel, where the series-series IPT (SS-IPT) system is commonly used in the current literature. The discussion in this paper is mainly based on the SS-IPT system. For most electrical applications and systems, load voltage (or power) control is the prime objective. A simple way to achieve IPT system output voltage regulation is to operate at an open-loop constant current or constant voltage mode [4-6], but in practical applications, operation condition variations, component tolerances and equivalent series resistances (ESRs) may affect the system output voltage level [7]. Adopting a proper closed-loop control is a common solution to enhance the IPT system adaptivity. For example, dual side DC-DC converters can provide high control flexibility in the closed-loop control [8]. The main disadvantages of using external DC-DC converters for voltage control includes the increment of system loss, circuit complexity, cost and size. To avoid the use of the additional DC-DC converters, one can also apply phase shift modulation (PSM) [9], pulse-width modulation (PWM) and

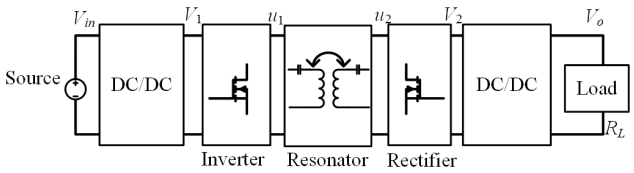

Fig. 1. A typical IPT system.

pulse density modulation (PDM) [10] methods to the inverter/rectifier to achieve system control. Unlike PSM and PWM that could result in a large efficiency drop due to hard switching, PDM is compatible with soft switching and thus the IPT system efficiency could remain at a high level [3]. However, for the load side, either implementing the aforementioned control methods on the rectifier or using an external DC-DC converter has a regulation capability limit that will restrict the transmission distance [11]. Performing front side voltage adjustment can extend the transmission distance, but dual-side information is usually required for a desirable cooperation control performance. Using communication modules is an ordinary solution, but the drawback is that the IPT system could suffer from a poor reliability and uncertain delays. Another method is to retrieve the secondary side information through waveform modulation instead of communication modules, e.g. [12]. Nonetheless, conventional waveform modulation methods prevent the system from staying at the optimum operating point and may exist hard switching, resulting in a lower efficiency. A large output capacitance may also be required to compensate the load voltage ripple. In this paper, a burst mode pulse density modulation (PDM) method is proposed to provide voltage regulation and signal feedback without communication modules. The method has the advantages of high efficiency, high reliability and large transmission distance.

II. PDM FOR VOLTAGE REGULATION

Fig. 2 illustrates the equivalent model of a SS-IPT system with R_1 and R_2 representing circuit ESRs. The magnetic coupler owns a primary self-inductance L_1, a secondary side self-inductance L_2 and a mutual inductance M. The mutual inductance M is related to the coil location, coil facing angle and coil structure. The external capacitors C_1 and C_2 are respectively the compensation capacitors for the front and load side. The

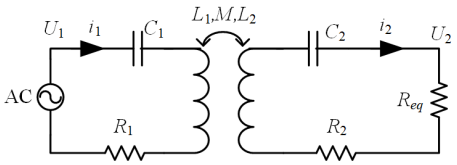

Fig. 2. Equipvalent SS-IPT model.

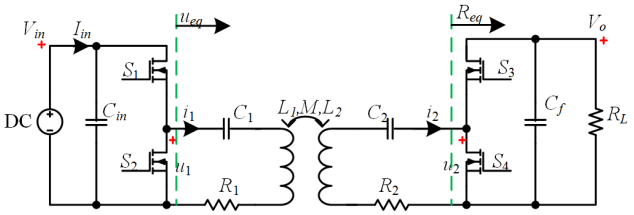

Fig. 3. An SS-IPT system with half-bridge converter.

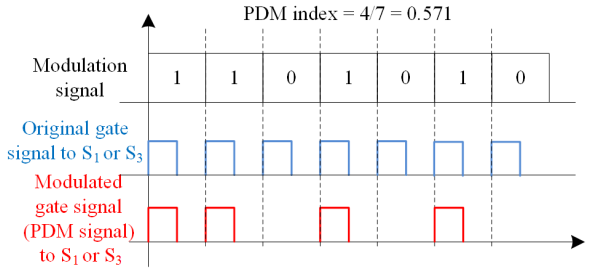

Fig. 4. PDM principle.

source U_1 and load R_{eq} represent the equivalent system input and output. Normally the SS-IPT system is designed to operate at the resonant frequency i.e.

$$\omega_s = \omega_1 = \omega_2 = \frac{1}{\sqrt{L_1 C_1}} = \frac{1}{\sqrt{L_2 C_2}} \tag{1}$$

where ω_s represents the system operating frequency. The primary and secondary side resonant frequencies ω_1, ω_2 are assumed to be identical for simplification. Following the analysis in [13], there is:

$$U_2 = \frac{j\omega_s M R_{eq} U_1}{R_1(R_2 + R_{eq}) + \omega_s^2 M^2} \approx \frac{jR_{eq}}{\omega_s M} U_1 \tag{2}$$

for $\omega_s^2 M^2 >> R_1(R_2+R_{eq})$. Hence, the equivalent load voltage U_2 will increase as the transmission distance or the coil misalignment increases.

The basic principle of PDM is to modulate the gate drive signals of the inverter/rectifier in order to provide an additional gain. Fig. 3 shows the circuit diagram of a dual active half-bridge IPT system. Taking the front side inverter as an example, in the normal operation, the switches S_1 and S_2 of the inverter will conduct alternately (ignoring deadtime) in every switching cycle. Under the PDM control shown in Fig. 4 [10, 14], when a '0' occurs in the modulation signal, S_2 will be on and S_1 will be off during the entire cycle. The density, or says percentage, of '1's in the modulation signal, is regarded as the PDM index '*d*', which is the control force. If the IPT system has a high quality factor and the '0's in the modulation signal is uniformly distributed, dual-side PDM in steady state can correspondingly provide:

$$V_o \propto d_1 V_{in} \tag{3}$$

$$R_{eq} = \frac{2}{\pi^2} d_2^2 R_L \tag{4}$$

where d_1 and d_2 are the pulse densities on the primary and secondary side respectively [3, 10]. The overall gains of the inverter G_1 and the rectifier G_2 are approximately given as:

$$G_1 = \frac{d_1\sqrt{2}}{\pi} \tag{5}$$

$$G_2 = \frac{\pi}{\sqrt{2} d_2} \tag{6}$$

Combining the results in (5), (6) with (2), one can get:

$$V_o = \frac{jR_L}{\omega_s M} V_{in} \frac{G_1}{G_2} = \frac{jR_L}{\omega_s M} V_{in} d_1 d_2 \frac{2}{\pi^2} \tag{7}$$

where R_L represents the actual load resistance. Equation (7) clearly shows that, when the coupling condition varies, the output voltage shall be regulated by controlling the converter gains. Load voltage regulation could be achieved locally in the secondary side by controlling d_2. However, due to the component stress, size and other consideration, there is always a regulation limit for a practical converter. Once the receiver coil is at a certain distance that the secondary side PDM reaches the regulation limit, the IPT system is regarded to be at the operation region boundary. Nonetheless, if the primary side converter adjusts d_1 properly, the secondary side voltage regulation could be restored and the power transmission range can be extended. As mentioned before, information exchange is generally required to achieve the dual side cooperation. The following section provides a method that could feedback a signal without the communication modules.

III. Burst Mode Control

The original burst mode operation is usually applied in the power factor correction (PFC) circuit for power consumption optimization under light or no load condition [15]. The burst mode operation mainly requires the system to switch between active mode and sleep mode to reduce switching loss.

In this paper, the burst mode operation is applied to the SS-IPT secondary side rectifier for signal feedback. In case of

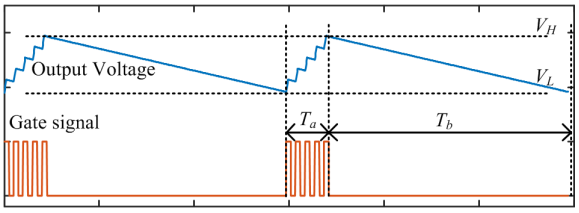

Fig. 5. Typicall burst mode operation.

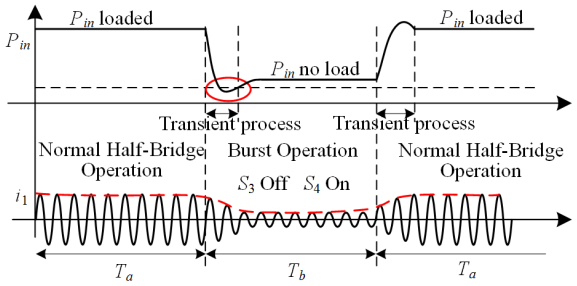

Fig. 6. Burst mode opertion in a SS-IPT system.

misunderstanding, the burst-on (on-time) and the burst-off (off-time) durations are denoted as 'T_a' and 'T_b', correspondingly. S_4 is on and S_3 is off for the period T_b, while the rectifier is in normal operation during T_a. Accordingly, the IPT system secondary side enters a no load state in T_b, where:

$$i_{1-noload} = \frac{u_1}{R_1 + \frac{\omega_s^2 M^2}{R_2}} \ll i_{1-loaded} = \frac{u_1}{R_1 + \frac{\omega_s^2 M^2}{R_{eq} + R_2}} \tag{8}$$

Equation (8) means that, during T_b, the primary side current in steady state is much smaller than the one in T_a, which further implies that the primary side resonator will discharge to the IPT system. Hence, the DC input power will drop to a distinctively low level during the transition as shown in Fig. 6. The significant power drop could be easily detected by the current sensor for I_{in}. In other words, the burst mode operation on the secondary side could feedback a signal to the primary side.

On the other hand, the burst mode operation will cause voltage variation on the load. According to the on-off keying (OOK) method [16] and the decoupler compensation one [2], there is:

$$R_{eq} = d\frac{2}{\pi^2}R_L \tag{9}$$

where $d=T_a/(T_a+T_b)$. Apparently, the burst mode operation equivalently introduces a gain on the rectifier that is different from the PDM one. To the best of the author's knowledge, the current literature mainly focuses on the voltage regulation ability of the burst mode control or other similar methods like OOK, but the signal feedback characteristic is not fully revealed.

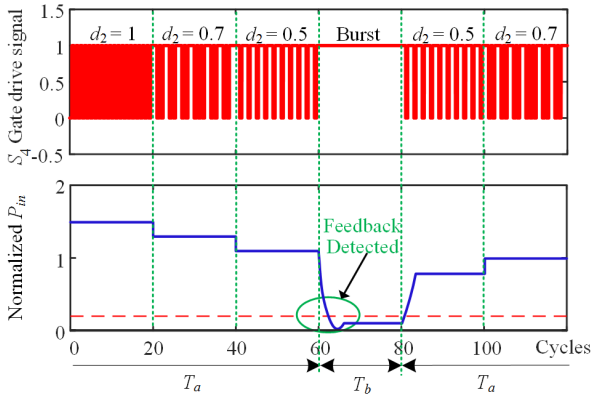

Fig. 7. Burst mode PDM principle.

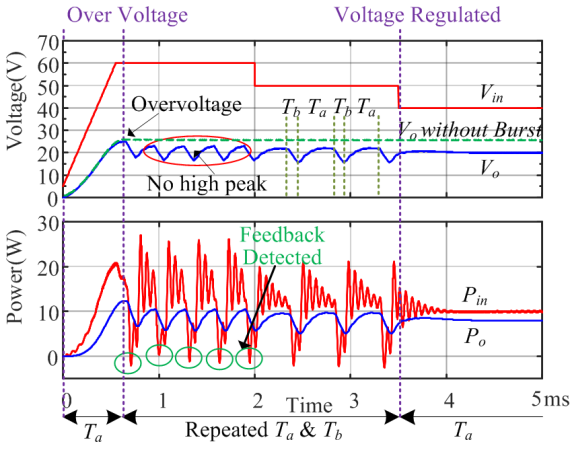

Fig. 8. Burst mode PDM simulation.

IV. Proposed Burst Mode PDM Control

In the proposed method, burst mode operation is applied to the secondary side converter to achieve signal feedback through waveform modulation. Therefore, no communication modules are required by the IPT system. Realizing that the burst mode control is highly compatible with PDM, the proposed system voltage regulation is based on PDM control to avoid using extra DC-DC converters. The proposed method utilizes the characteristics of the burst mode operation and the PDM such that: (1) An overvoltage signal is fed back to the front side controller without communication modules; (2) Burst mode operation provides extra voltage regulation for output protection; (3) The IPT system operates under PDM control in steady state for a high efficiency.

Fig. 7 demonstrates the burst mode PDM process. At the beginning of Fig. 7, the receiver is already out of the critical range, and the secondary PDM pulse density d_2 soon reaches the minimum value 0.5. The front side should be notified to change the input voltage to maintain the load voltage level. The burst mode operation turns on S_4 and turns off S_3 for a long duration and the system enters T_b that: (1) The input power experiences a drop due to the receiver side burst operation, which can be detected by measuring the input side DC current; (2) The input

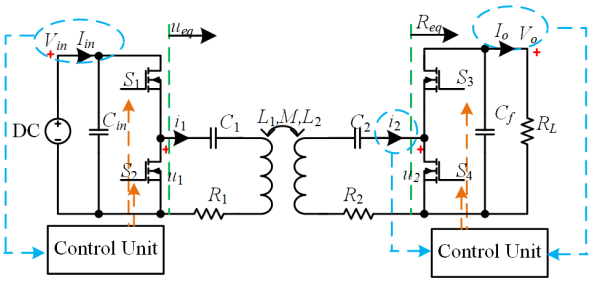

Fig. 9. Proposed SS-IPT System.

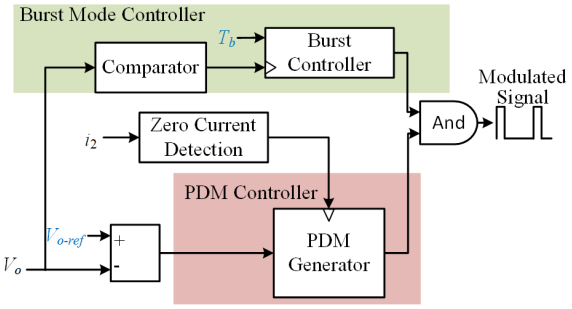

Fig. 10. Secondary side controller diagram.

voltage reduces by a pre-defined value once the power drop is sensed; (3) The inverter filter capacitor discharges to the load and the output voltage remains in a suitable region. From the capacitor discharging formula $\Delta V_o \approx I_o \Delta t / C_f$, the duration of T_b is put to a constant, which can be determined from the allowed output voltage drop (or says ripple percentage). The quantitative gain analysis of the burst mode operation may refers to (2) and (9) or [16]. Afterward, the secondary PDM controller slowly restores the output voltage. Note that setting d_2 to be fixed at 0.5 can increase system stability while using the PDM index given by the secondary controller, such as a PI controller, provides a faster voltage restoration speed. However, if the system input is still excessive, the load voltage will exceed the voltage limit and another 'burst' will be triggered to send back an overvoltage signal and reduce the load voltage. The input voltage is thus adjusted to a suitable level that the output regulation can be achieved. There is no burst operation after the completion of input adjustment. From the above analyses, the proposed burst mode PDM control can achieve signal feedback and provide a load voltage protection. The overall efficiency is not affected by the burst mode operation as the system is under PDM control for most of the time.

The proposed IPT system structure is depicted in Fig. 9. Fig. 10 shows one example controller schematic for the proposed method. The burst mode control block is like a peripheral module to the PDM generation block. When the secondary side loses regulation capability, the comparator block will trigger the burst mode controller. Other structures such as triggering the burst mode module by the PDM saturation signal are also possible. A complete simulation with the receiver placed outside the critical range is given in Fig. 8 to illustrate the entire process. The dash curve indicates that the output voltage without the burst operation will be larger than the desired value 20 V. The input side is deliberately designed to ignore the current (power) drop for multiple times so as to show that, even if the input side

TABLE I. EXPERIMENT PROTOTYPE PARAMETERS

Symbol	Description	Value
L_1	Primary side inductor	~75.3 μH
L_2	Secondary side inductor	~75.3 μH
C_1	Primary side capacitor	400 pF
C_2	Secondary side capacitor	400 pF
R_1	Primary side ESR	~ 0.7 Ω
R_2	Secondary side ESR	~ 0.7 Ω
C_f	output filter capacitor	3.2 μF
k	coupling coefficient	~0.05
f_s	switching frequency	~0.909 MHz

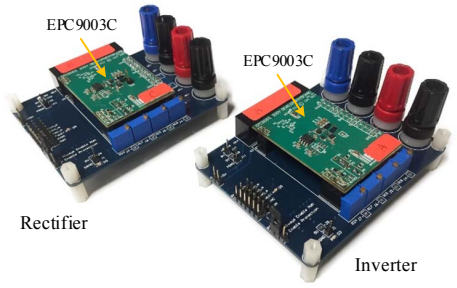

Fig. 11. Inverter and rectifier [3].

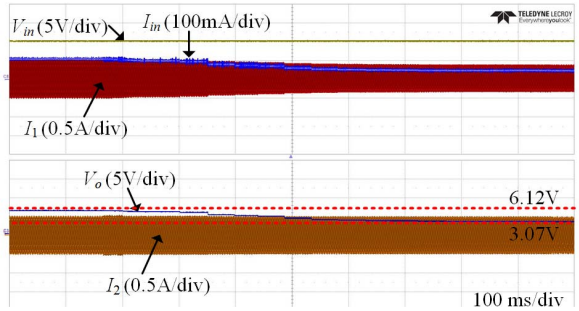

Fig. 12. Experiment result for PDM.

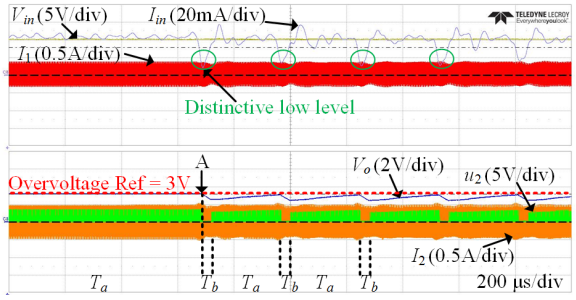

Fig. 13. Experiment result for burst mode PDM.

responds very slowly or cannot recognize the feedback, the secondary side voltage is always inside a safe zone. At 2 ms, the primary voltage is reduced by 10 V after the feedback signal recognition. However, the load side is still in an over-voltage (PDM saturation) status and hence the burst mode operation continues. The primary voltage then decreases to 40 V (67% of the original value) and the load voltage is regulated by the PDM

controller successfully. The whole system operates under PDM control after the completion of primary voltage adjustment.

V. Experimental Verification

An experimental prototype following the schematic in Fig. 3 is used with the system parameters listed in Table I. The two EPC9003C boards in Fig. 11 are used as the inverter and rectifier. The DC input voltage is set to be 10 V and the load resistance is 50 Ω, while an output voltage above 3 V is regarded as overvoltage.

The experiment in Fig. 12 verified the PDM control voltage regulation capability. When there is no control action at the beginning, the output voltage is at 6 V. With the reduction of d_2, the output voltage is finally regulated to 3 V, corresponding to the pre-defined minimal PDM pulse density 0.5. As discussed above, unless the input voltage level is reduced, the system shall not be allowed to operate under a smaller coupling coefficient to prevent loss of control. Fig. 13 illustrates the signal feedback and voltage regulation capabilities of the burst mode PDM method. Note that before point A, the burst mode operation control is intentionally disabled to show the difference. In this experiment, T_b is set to 30 cycles (30 μs) that $\Delta V_o \approx 0.65$ V. The distinctive drops in the input current are clearly shown. Meanwhile, it can be seen that the output voltage is maintained under 3 V for all T_b and T_a periods. The experiment shows that the burst mode PDM method can achieve output protection at overvoltage condition and the overvoltage signal feedback.

VI. Conclusion And Future Work

In this paper, a burst mode PDM method is presented and verified by both simulation and experiment. The burst mode PDM method achieves dual-side cooperation without using communication modules. In normal operation, the proposed method performs system control as the ordinary PDM method and a high overall efficiency is hence achievable. When the secondary side reaches regulation limit, the burst mode operation is triggered to inform the front side so as to adjust input voltage. The burst mode operation also provides overvoltage protection. The voltage regulation capability is hence restored and the operation region is extended. Compared to the basic method requiring communication modules and DC-DC converters, the main advantages of the proposed method are that, the system complexity, cost and size are reduced while the system reliability is enhanced. Future work includes a completed experiment with efficiency and more data as well as a further analysis of the burst mode PDM method.

References

[1] G. A. Covic and J. T. Boys, "Inductive Power Transfer," *Proceedings of the IEEE,* vol. 101, pp. 1276-1289, 2013.

[2] J. T. Boys and G. A. Covic, "The Inductive Power Transfer Story at the University of Auckland," *IEEE Circuits and Systems Magazine,* vol. 15, pp. 6-27, 2015.

[3] H. C. Li, J. Y. Fang, S. X. Chen, K. P. Wang, and Y. Tang, "Pulse Density Modulation for Maximum Efficiency Point Tracking of Wireless Power Transfer Systems," *IEEE Transactions on Power Electronics,* vol. PP, pp. 1-1, 2017.

[4] W. Zhang and C. C. Mi, "Compensation Topologies of High-Power Wireless Power Transfer Systems," *IEEE Transactions on Vehicular Technology,* vol. 65, pp. 4768-4778, 2016.

[5] R. Mai, Y. Chen, Y. Li, Y. Zhang, G. Cao, and Z. He, "Inductive Power Transfer for Massive Electric Bicycles Charging Based on Hybrid Topology Switching With a Single Inverter," *IEEE Transactions on Power Electronics,* vol. 32, pp. 5897-5906, 2017.

[6] X. Qu, H. Han, S. C. Wong, C. K. Tse, and W. Chen, "Hybrid IPT Topologies With Constant Current or Constant Voltage Output for Battery Charging Applications," *IEEE Transactions on Power Electronics,* vol. 30, pp. 6329-6337, 2015.

[7] A. Costanzo, M. Dionigi, F. Mastri, M. Mongiardo, G. Monti, J. A. Russer*, et al.*, "Conditions for a Load-Independent Operating Regime in Resonant Inductive WPT," *IEEE Transactions on Microwave Theory and Techniques,* vol. 65, pp. 1066-1076, 2017.

[8] H. Li, J. Li, K. Wang, W. Chen, and X. Yang, "A Maximum Efficiency Point Tracking Control Scheme for Wireless Power Transfer Systems Using Magnetic Resonant Coupling," *IEEE Transactions on Power Electronics,* vol. 30, pp. 3998-4008, 2015.

[9] Z. Ye, P. K. Jain, and P. C. Sen, "A Full-Bridge Resonant Inverter With Modified Phase-Shift Modulation for High-Frequency AC Power Distribution Systems," *IEEE Transactions on Industrial Electronics,* vol. 54, pp. 2831-2845, 2007.

[10] H. C. Li, J. Y. Fang, and Y. Tang, "Delta-Sigma Modulation for Maximum Efficiency Point Tracking of Wireless Power Transfer Systems," *2017 IEEE 3rd International Future Energy Electronics Conference (IFEEC-ECCE Asia), KaohSiung, 2017*.

[11] H. C. Li, Y. Tang, K. P. Wang, and X. Yang, "Analysis and control of post regulation of wireless power transfer systems," in *2016 IEEE 2nd Annual Southern Power Electronics Conference (SPEC)*, 2016, pp. 1-5.

[12] W. Zhong and S. Y. R. Hui, "Charging Time Control of Wireless Power Transfer Systems Without Using Mutual Coupling Information and Wireless Communication System," *IEEE Transactions on Industrial Electronics,* vol. 64, pp. 228-235, 2017.

[13] W. Zhang, S. C. Wong, C. K. Tse, and Q. Chen, "Design for Efficiency Optimization and Voltage Controllability of Series–Series Compensated Inductive Power Transfer Systems," *IEEE Transactions on Power Electronics,* vol. 29, pp. 191-200, Jan. 2014.

[14] H. Y. Leung, D. Mccormick, D. M. Budgett, and A. P. Hu, "Pulse density modulated control patterns for inductively powered implantable devices based on energy injection control," *IET Power Electronics,* vol. 6, pp. 1051-1057, 2013.

[15] Y. K. Lo, S. C. Yen, and C. Y. Lin, "A High-Efficiency AC-to-DC Adaptor With a Low Standby Power Consumption," *IEEE Transactions on Industrial Electronics,* vol. 55, pp. 963-965, 2008.

[16] W. Zhong and S. Y. R. Hui, "Maximum Energy Efficiency Operation of Series-Series Resonant Wireless Power Transfer Systems Using On-Off Keying Modulation," *IEEE Transactions on Power Electronics,* vol. PP, pp. 1-1, 2017.